AD-A270 599

Naval Research Laboratory

Washington, DC 20375-5320

NRL/MR/5915/93-7319

SURFACE IMPEDANCE MODIFICATION OF PLATES IN A WATER-FILLED WAVEGUIDE

DTIC
ELECTE
OCT 14 1993
S A D

Pieter S. Dubbelday

Naval Research Laboratory
Underwater Sound Reference Detachment
P.O. Box 568337, Orlando, FL 32857-8337

15 September 1993

93-24118

Approved for public release; distribution unlimited.

REPORT DOCUMENTATION PAGE

Form Approved
OMB No. 0704-0188

Public reporting burden for this collection of information is estimated to average 1 hour per response, including the time for reviewing instructions, searching existing data sources, gathering and maintaining the data needed, and completing and reviewing the collection of information. Send comments regarding this burden estimate or any other aspect of this collection of information, including suggestions for reducing this burden, to Washington Headquarters Services, Directorate for Information Operations and Reports, 1215 Jefferson Davis Highway, Suite 1204, Arlington, VA 22202-4302, and to the Office of Management and Budget, Paperwork Reduction Project (0704-0188), Washington, DC 20503.

1. AGENCY USE ONLY *(Leave blank)*	2. REPORT DATE	3. REPORT TYPE AND DATES COVERED
	15 September 1993	FINAL

4. TITLE AND SUBTITLE
Surface Impedance Modification of Plates in a Water-Filled Waveguide

5. FUNDING NUMBERS
PE - 61153N
TA - RR011-08-42
WU - DN580-030

6. AUTHOR(S)
Pieter S. Dubbelday

7. PERFORMING ORGANIZATION NAME(S) AND ADDRESS(ES)
NAVAL RESEARCH LABORATORY
UNDERWATER SOUND REFERENCE DETACHMENT
PO BOX 568337
ORLANDO, FL 32856-8337

8. PERFORMING ORGANIZATION REPORT NUMBER
NRL MEMORANDUM REPORT 7319

9. SPONSORING/MONITORING AGENCY NAME(S) AND ADDRESS(ES)
OFFICE OF NAVAL RESEARCH
800 N. QUINCY STREET
ARLINGTON, VA 22217-5000

10. SPONSORING/MONITORING AGENCY REPORT NUMBER

11. SUPPLEMENTARY NOTES

12a. DISTRIBUTION/AVAILABILITY STATEMENT
Approved for public release; distribution unlimited.

12b. DISTRIBUTION CODE

13. ABSTRACT *(Maximum 200 words)*

The interaction of plane waves, propagating in a water-filled cylindrical waveguide with a plate perpendicular to its axis, with the same cross section as the tube, is determined by the surface impedance at the plate relative to the specific acoustic impedance of the medium. By means of an attached piezoelectric disk-shaped double transducer (sensor and actuator) the apparent surface ijmpedance of the combination may, in principle, be modified to equal the impedance of the medium, thus establishing a no-reflection situation. The actuator voltage is regulated by feedback loop, based on an algorithm for complex-root finding. The analysis of this concept is given and a figure-of-merit for the transducer material is presented. Efforts to demonstrate experimentally the feasibility of this concept were inconclusive.

14. SUBJECT TERMS	15. NUMBER OF PAGES
Surface impedance modification Active termination in waveguide No-reflection condition	31
	16. PRICE CODE

17. SECURITY CLASSIFICATION OF REPORT	18. SECURITY CLASSIFICATION OF THIS PAGE	19. SECURITY CLASSIFICATION OF ABSTRACT	20. LIMITATION OF ABSTRACT
UNCLASSIFIED	UNCLASSIFIED	UNCLASSIFIED	UL

NSN 7540-01-280-5500

Standard Form 298 (Rev 2-89)
Prescribed by ANSI Std 239-18
298-102

BLANK PAGE

CONTENTS

Accesion For

NTIS CRA&I ☑
DTIC TAB ☐
Unannounced ☐
Justification

By
Distribution /

Availability Codes

Dist	Avail and / or Special
A-1	

DTIC QUALITY INSPECTED 8

BLANK PAGE

SURFACE IMPEDANCE MODIFICATION OF PLATES IN A WATER-FILLED WAVEGUIDE

INTRODUCTION

The guidance and control of acoustic waves in a fluid medium may be accomplished by means of passive materials that are able to transmit, reflect, and absorb acoustic radiation in varying degrees. There are limitations to the best of designs using passive materials. Active materials offer the possibility of expanding the range of control. They appear especially to hold promise at low frequencies, where passive materials may lead to unwieldy size.

During the past decade, the interest, research, and industrial applications of active control have increased considerably, especially in the field of active noise control. It is impossible within the confines of this report to give even a modest introduction to the relevant literature. Therefore, the reader is referred to the lists of references in the articles given below, and especially to the reference bibliography by Guicking [1]. Fundamental concepts of active sound control are discussed by Ffowcs-Williams [2] and Scheuren [3,4].

A good general introduction in textbook style to the subject of active control of sound is the monograph by Nelson and Elliott [5]. It gives an extensive discussion of interference of plane-wave sound fields in wave guides, with special emphasis on the question of where the power in the field is created and absorbed (Chapter 5). In connection with the treatment of an absorbing termination at the end of a duct by means of a secondary source, the authors mention the work of Bobber and others at the Naval Research Laboratory, USRD. The fundamental properties of such a system were investigated by Bobber [6,7] and Beatty [8]. These studies were applied to test sonar transducers under traveling-wave conditions in a tube filled with a

Manuscript approved 21 June 1993

liquid at high pressure [9]. For the continuation of this type of system in air, Nelson and Elliott refer to the work of Guicking et al. [10,11]. Adaptive control of such a system is discussed by Orduña-Bustamante and Nelson [12].

In all these investigations, it is typical that the probing of the acoustical field is accomplished by sensors that are placed in the field well away from the actuator surface. In contrast to this arrangement it is attempted in the present study to influence the reflection of waves by a plate in a water-filled waveguide by means of layers of active material attached to the plate. Thus, the complete arrangement of sensor(s) and actuator is designed to have a thickness that is (much) smaller than the lateral extension of the plate, in accordance with the popular notion of a "smart skin".

In a previous study [13], a no-transmission experiment in a water-filled waveguide was reported. The wave, passing through a single layer of active material (actuator), is suppressed by regulating the voltage of the actuator through a feedback loop that reduces the voltage output of a sensor placed behind the plate to zero. The feedback loop is closed by a computer, which performs its task by means of an algorithm from complex-root-finding concepts.

Suppressing the wave reflected by a plate is more involved, since one needs two items of information, in order to separate the amplitude of the reflected wave from that of the incoming wave [14]. These could be derived from two pressure transducers, or from one pressure transducer and one velocity transducer. It might be expected that one would need one more transducer yet, acting as an actuator, in order to produce the proper acoustic wave to interfere with the incoming wave. In the analysis presented here it is shown that one may establish a no-reflection condition by means of only two active layers attached to the plate. The voltage of one of these, the actuator, is governed by a feedback loop based on the same algorithm as referred to above, which uses the voltage signal from the other layer, the sensor.

Two aspects may be distinguished: first, the use of a feedback method based on the technique of complex root-finding; and, second, a mathematical

analysis that shows how a combination of one sensor and one actuator leads to an operable feedback loop by means of this algorithm.

After a description of the equipment, an analysis is presented to show the intended operation of the double transducer. Next, experiments are discussed that were designed to show the feasibility of the concept.

WAVEGUIDE AND TRANSDUCERS

A sketch of the waveguide used in this experiment is shown in Fig. 1. This is an NRL-USRD (Naval Research Laboratory, Underwater Sound Reference Detachment) type G19 calibrator [15]. A plane wave is created in the water-filled tube by a coil-driven piston in the bottom. Reflection of this wave by the free surface leads to a standing-wave pattern. In its original form, the tube wall was made of aluminum. In most of the following experiments, a polymethylmethacrylate (indicated by the trade name lucite) tube was used. This (transparent) waveguide was originally designed for laser Doppler experiments.

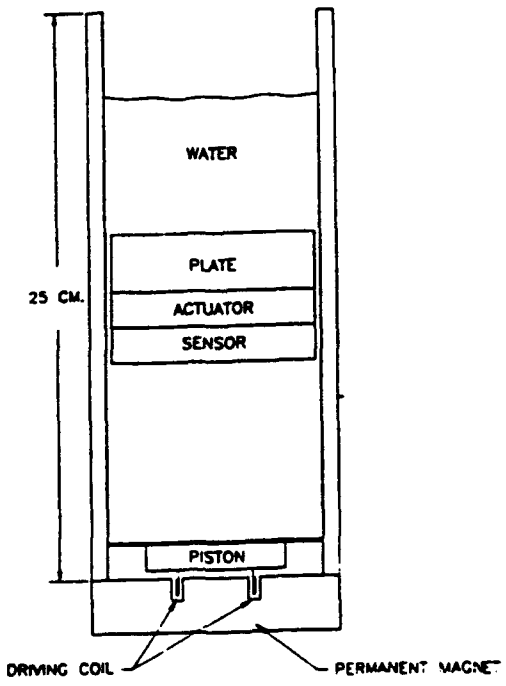

Fig. 1 - Experimental arrangement in G19 calibrator.

The wave speed in the medium contained in the calibrator (water) is not equal to the wave speed in a medium of unlimited extent due to the elasticity of the tube wall. To establish the character of the field in the calibrator, the pressure near the piston s_c was measured by an LC5 (Atlantic Research) miniature hydrophone, and the velocity v_c was determined from the response of an accelerometer mounted on the side of the piston opposite to the water column. From these measurements, one may compute the specific impedance z_c seen by the piston by $z_c = p_c/v_c$.

The results are shown in Fig. 2, for a water column of 20.3 cm height in the calibrator. The magnitude of the impedance is given as a function of the frequency. The solid line connects the experimental points indicated by squares.

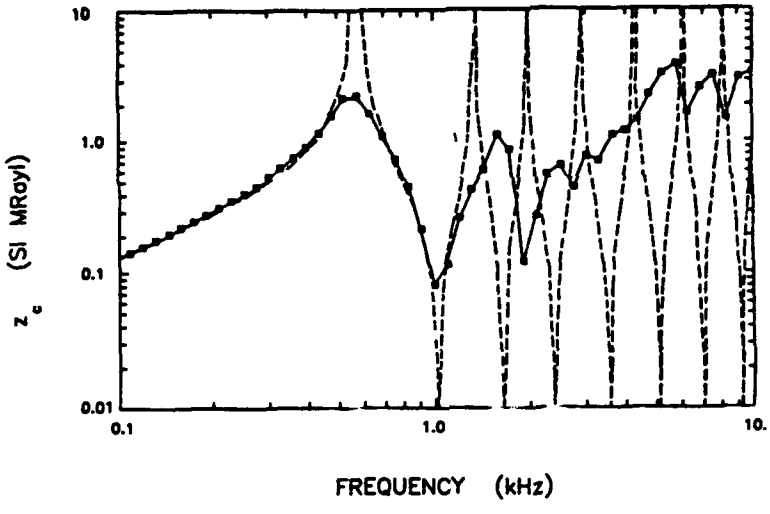

Fig. 2 - Specific impedance z_c at piston surface as a function of frequency. Solid curve: computed from measured pressure and velocity at piston. Dashed curve: according to standing wave value $z_c = \rho_o c_o \tan k_o h$, where c_o is evaluated for a water-filled infinite elastic cylinder.

The dashed line represents the theoretical impedance $\rho_o c_o \tan k_o h$ for a water column of height h, with a pressure release surface at one end; where ρ_o is the density of the water and $k_o = w/c_o$. The propagation speed c_o is computed from a model for axially symmetric propagation of waves in an infinite water-filled circular elastic cylinder [16]. The ratio of outer to

inner radius of the tube is 1.125, the inner radius is 10.2 cm, the height of the water column is 20.3 cm, the density of the wall material (lucite) is 1200 kg/m^3, its Young's modulus is 4.74 GPa, and its Poisson's ratio is 0.316 (from Ref.17).

Because the cross-sectional areas of piston and tube are not equal, the theoretical impedance was normalised such that it coincided with the experimentally measured impedance at the low-frequency end (see Fig.2). The factor used was 0.3, not far from the ratio 0.4 of the areas of the piston and tube cross sections. One sees that the first antiresonance at 550 Hz and the first resonance at 1000 Hz are well approximated by the model. At higher frequencies the correspondence between experiment and theory appears to be lost.

To analyse this effect, the wave speed was computed from the experimental frequency of the resonances and antiresonances at those locations where they appeared well resolved. This is compared with the computed wave speed as a function of frequency shown in Fig. 3. As expected, the points from the first antiresonance and from the first resonance are close to the theoretical curve, but the points from the next three features do not show close correspondence. The experimental points do indicate some decrease of wave speed with frequency, but they do not confirm the strong dispersion predicted by the model above about 1000 Hz. The cause of this discrepancy is not known.

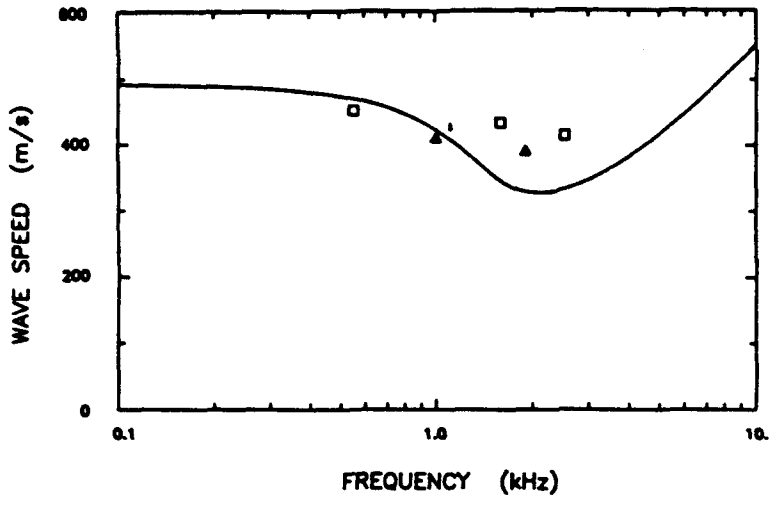

Fig. 3 - Solid curve: computed wave speed c_o of axially symmetric waves in a water-filled infinite wave guide with elastic cylindrical wall.
Points: [] - computed from antiresonance frequencies in experimental curve (solid curve in Fig.2).
Δ - computed from resonance frequencies in experimental curve (solid curve in Fig.2).

The double transducer (Fig. 4) is constructed from two layers of active material, each 3.3 mm thick. The active material is NTK Piezorubber PR-306. ("Piezorubber" is a trademark of NTK Technical Division, NGK Spark Plug Co., Nagoya, Japan.) It consists of $PbTiO_3$ particles embedded in a neoprene elastomer matrix. The center electrode is common to both transducer disks, and is kept at ground potential. The shields of the transducers and the shields of the coaxial cables are electrically connected together and to ground. The polarisation of the two transducers is antiparallel.

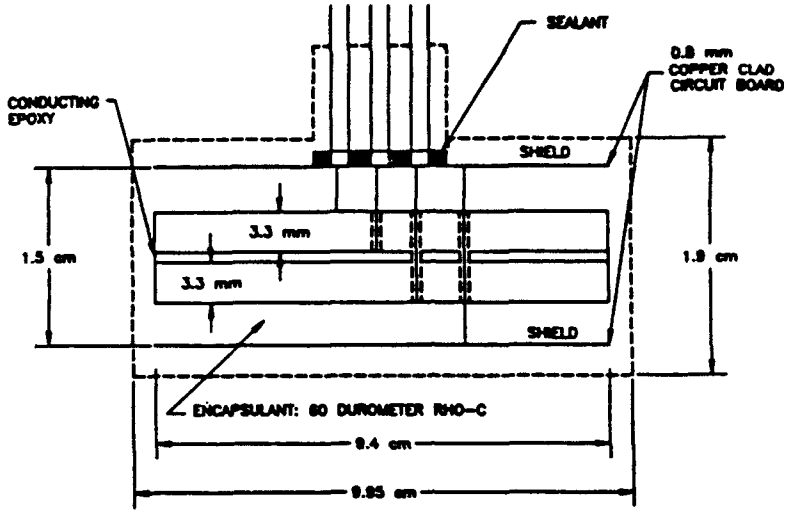

Fig. 4 - Sketch of cross section of double transducer.

FEEDBACK ALGORITHM

The feedback algorithm used in this experiment is more extensively discussed in Ref.13. It is based on the observation that the purpose of the adaptive feedback arrangement is to reduce an observable quantity, or an expression in terms of observable quantities, to zero. In the case of a no-transmission condition the observable quantity is simply the output voltage of a sensor placed behind the plate, the transmission of which should be suppressed. For a no-reflection condition, an expression in terms of observable quantities is involved, as discussed below. In any case, this expression in terms of observed quantities may be considered as the dependent variable w of an analytic complex function w. The independent variable of this complex function is the input voltage to the actuator z. The feedback algorithm follows from the notion that the desired result is equivalent to finding the root of the complex function $w = f(z)$. The root finder used in the present investigation is the complex equivalent of the secant method in real analysis.

In this root-finding method one starts with two pairs of variables, (z_1,w_1) and (z_2,w_2), for two arbitrary voltage inputs z_1 and z_2 to the actuator, corresponding to two values w_1 and w_2 computed from the observed sensor voltages. A new actuator voltage z_3 is computed by $z_3 = (w_2z_1 - w_1z_2)/(w_2-w_1)$. This process is repeated by observing the corresponding sensor voltage and computing the output function w_3. The next iteration is started by setting $z_2 \rightarrow z_1$, $w_2 \rightarrow w_2$, $z_3 \rightarrow z_2$, and $w_3 \rightarrow w_2$. The procedure is continued until the "cost function" $|w|$ is below a certain preset low value.

MODEL FOR OPERATION OF DOUBLE TRANSDUCER

Unlike the suppression of a transmitted wave described in Ref. 13, it is necessary for the intended suppression of a reflected wave to rely upon a mathematical model and the knowledge of certain material parameters of the active material. The model for one-dimensional wave propagation in the wave guide used here is discussed in detail in Appendix A. In the following discussion the definitions and results of Appendix A will be used.

It is assumed that the two elastic layers are made of the same material and have equal thicknesses. This is not an essential restriction, but it simplifies the analysis and offers better insight into the physics of the problem. Results for the relations between variables for the general case of unequal layer parameters may be found in Ref. 18. The model shows that the set of eight unknowns, namely the forces per unit area and the velocities at the interfaces at both sides of each of the two active layers, may be related to the controlled or observable quantities: the voltages of actuator and sensor, and the current through the actuator.

The algebra gives the result, not surprising, that the current through the actuator is mostly due to the capacitance of the actuator disk, and is little affected by the details of the acoustic impedances. This puts excessive demands on the accuracy of the current meter. Therefore, a different approach is followed.

One observes the two voltages V_{10} and V_{20} of actuator and sensor, while there is no external voltage impressed on the actuator and the terminals are open-circuited. Under these conditions the actuator current density J_1 is known, since it is zero, and one can find the forces and velocities at the two exterior surfaces of the double transducer. Two of these are given here,

$$f_{21} = z_{11} \frac{(V_{10}+V_{20}) + (V_{10}-V_{20})(1+\cos kd)/\cos kd}{2z_{13}} \tag{1}$$

and

$$v_{21} = \frac{(V_{10}+V_{20}) - (V_{10}-V_{20})\cos kd/(1-\cos kd)}{2z_{13}} , \tag{2}$$

where $z_{11} = \rho c /(i \tan kd)$; ρ is the density and c the propagation speed in the transducer material; $k = \omega/c$, d the transducer thickness; $z_{13} = h_{33}/(i \omega)$; and h is the piezoelectric constant.

The impedance z_p presented to the wave by the plate is given by the ratio of force and velocity at the interface with the plate; thus, $z_p = -f_{21}/v_{21}$. Then z_p may be expressed in terms of a non-dimensional impedance z_p' defined by $z_p = z_p' z_d$, where z_d is related to the parameters of the layers by $z_d = i \rho c \tan(kd/2)$, in the following form

$$z_p' = \frac{(V_1+V_2) \cos kd + (V_1-V_2)(1+\cos kd)}{(V_1+V_2)(1-\cos kd) - (V_1-V_2) \cos kd} . \tag{3}$$

For small values of kd (this condition is satisfied in the experiments described below), the expression for z_p simplifies to

$$z_p \simeq 0.5 \; i \; \omega\rho d \frac{-3V_1+V_2}{V_1 - V_2} . \tag{4}$$

It would appear reasonable to assume that this impedance is constant for a long period of time (long as compared with the time needed to establish the desired no-reflection condition), and thus, once computed it remains available during further measurements and computations. One may observe in Eq.(3) that the only material constants needed in the computation of the plate impedance are the propagation speed of plane waves (needed for computing the wave number k) and the density of the plate material (in the definition of z_d). When kd is small Eq.(4) is obtained, and only the piezorubber density is required in addition to the layer thickness, both easily measured quantities.

For the next step one impresses a voltage on the actuator. Returning to the set of equations A1-A6, the measured z_p now provides a relation between force and velocity at the plate. Thus, the number of unknowns reduces by one, and J_1 may be left unobserved. The algebra again gives the various unknown quantities expressed in terms of V_1, V_2, and z_p. The results are given in Appendix A. The expressions are rather complicated, but it suffices to notice that the surface impedance of the sensor $z_e = f_{12}/v_{12}$ may be expressed in terms of the impressed actuator voltage and observed sensor voltage, in addition to the previously determined plate impedance z_p.

The feedback arrangement reduces here to the problem of finding an actuator voltage such that the difference between the value of z_e and a desired impedance z_i is reduced to zero. For a no-reflection condition the value of z_i should be $\rho_o c_o$, where the subscript zero refers to the values of density and propagation speed of the medium, which in an elastic waveguide is affected by the elasticity of the wall. The relevant function w may be written in a more practical form by

$$w = f_{12} - z_i v_{12} \cdot \qquad (5)$$

The feedback loop is designed to find an actuator voltage V_1 such that the absolute value of this function w (the "cost function" in control theory language) is decreased as much as possible, ideally to zero.

In principle one may dial any desired impedance z_i. For instance, $z_i = 0$ would impose a pressure release condition and $z_i \to \infty$, equivalent to $v_{12} = 0$, amounts to a velocity release surface.

EXPERIMENTS

The experiments were performed according to the analysis presented before, in the arrangement sketched in Fig.1. The experiments were done with and without a backing plate behind the double transducer. The operation of the feedback loop worked satisfactorily. Convergence to the desired condition was reached in about three steps. Unfortunately, an important criterion for the correctness of the experiment failed to be satisfied.

A no-reflection condition established at the plate by the double transducer necessarily affects the impedance seen by the piston. Specifically, the impedance of the water column at the piston should be equal to $\rho_o c_o$, the specific acoustic impedance of the medium. Notice that c_o is not the sound speed of the free medium, but is influenced by the elasticity of the walls of the calibrator, as discussed above. Moreover, a correction factor is needed to account for the fact that the piston area is smaller than the cross-sectional area of the tube. It is assumed that the evanescent waves connected with satisfying the boundary condition at the piston have little effect. The specific impedance at the piston was measured by means of a miniature hydrophone located close to the center of the piston, and an accelerometer mounted on the back side of the piston. In all cases there was a discrepancy of at least an order of magnitude between the impedance measured directly in this fashion and the impedance $\rho_o c_o$ entered into the computer program governing the feedback loop.

To investigate the source of this discrepancy, the pressure and velocity at the surface of the double transducer (without backing plate) oriented towards the free water surface were measured by the miniature hydrophone and an accelerometer (Fig. 5). This was compared with the values computed from the observed V_1 and V_2 of the actuator and sensor when no external voltage was impressed on the actuator. A typical example is shown in Figs. 6 and 7. It was somewhat encouraging that the general trend in the directly measured values of pressure and velocity was followed by the values computed from the double transducer. The difference in the magnitude is very large, though.

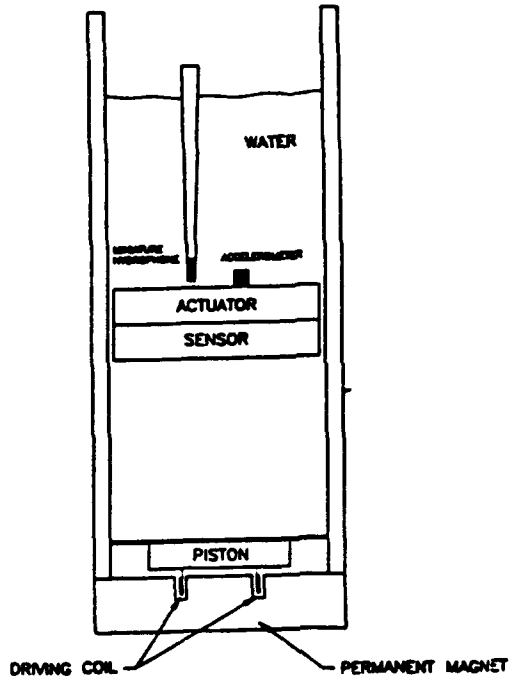

Fig. 5 - Sketch of setup for comparison of pressure and velocity computed from voltages of double transducer (no current) with pressure from miniature hydrophone and velocity from accelerometer.

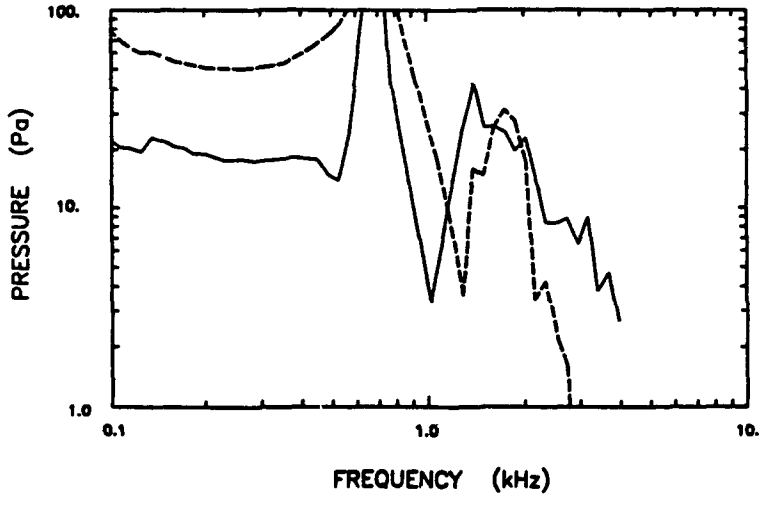

Fig. 6 - Comparison of the pressure as a function of frequency at the transducer face opposite to the incoming wave computed from voltages in double transducer (solid line) with the measurement by a hydrophone (dashed line).

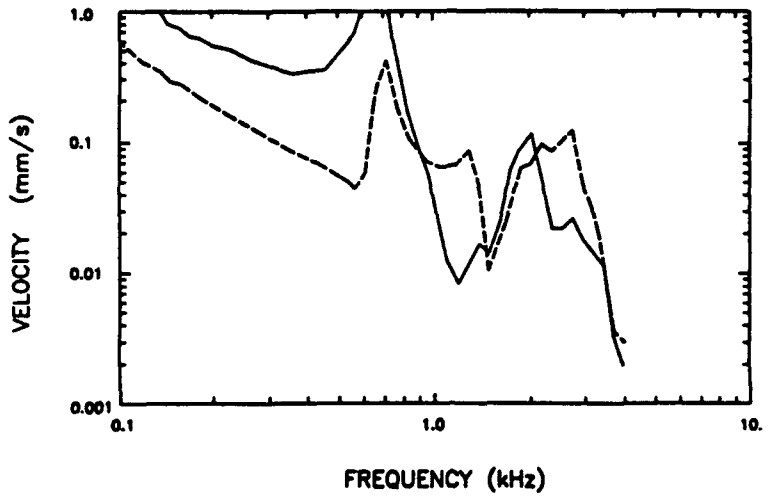

Fig. 7 - Comparison of the velocity as a function of frequency at the transducer face opposite to the incoming wave computed from voltages in double transducer (solid line) with the measurement by an accelerometer (dashed line).

Extensive study was made of the possible sources for this discrepancy. To exclude possible effects of propagation in the walls of the tube, an experiment was set up whereby a double transducer without encapsulant was directly placed on a shaker in air. Even in this simplified case the ratio of values for the two voltages V_1 and V_2 could not be reconciled with the value computed from Eq. (B4).

It was concluded at last that, most probably, the discrepancy is not due to any errors in the experiment or analysis. Instead, it appears that the problem is due to deviations in the actual wave action in the transducer from the simple one-dimensional description represented in the model. The finite size of the transducer disks allows other modes than just a pure thickness vibration to enter the picture, and this may couple into the voltage measured across the transducer.

In Ref. 20 an experiment with a single piezoelectric transducer mounted on a shaker is described. The authors discuss problems with discrepancies between experiment and analysis that are due to deviations from one-dimensional wave propagation. They found that very careful design of the transducer and choice

of a specific piezorubber are required to obtain results that concur with the assumed one-dimensional theory. Further discussions with one of the authors (M.D. McCollum) supported the diagnosis that the discrepancies in the study reported here also stem from deviations from one-dimensional wave theory.

FIGURE-OF-MERIT FOR NO-REFLECTION EXPERIMENT

In Appendix B, a derivation is given for a figure-of-merit (FOM) in the no-reflection experiment. It is assumed that the transducer layers are thin, i.e., kd << 1. For both steps in the experiment the proper expression is FOM = $d\ h_{33} / c_{33}^{D}$. In Table 1 values of piezoelectric coefficients are given, obtained from the literature, with the values of the FOM computed for d = 3.175 mm (1/8") for various active materials.

Table 1. FOM for no-reflection experiment; FOM = $d\ h_{33} / c_{33}^{D}$. It is assumed that the thickness d is 3.175 mm (1/8").

Material	h_{33} (GV/m)	c_{33}^{D} (GPa)	FOM (mV/Pa)
PZT5	2.15	147.	0.046
$BaTiO_3$	1.56	171.	0.029
PVDF	0.97	9.3	0.33
PR 305	0.46	2.4	0.608
PR 306	0.38	6.4	0.188

CONCLUSIONS

For the case of a no-reflection experiment, the feedback algorithm, based on a complex root-finder, works properly.

The analysis of the arrangement of two active layers attached to a backing plate shows that it is theoretically possible to establish a no-reflection condition by means of feedback.

The attempts to experimentally demonstrate the feasibility of this concept were inconclusive, presumably due to deviations from the one-dimensional wave-propagation theory implicit in the model.

ACKNOWLEDGEMENTS

The author wishes to express his thanks to Mr. Robert Voor for his assistance with the measurements and computer programming. This work was supported by the Office of Naval Research.

REFERENCES

1. D. Guicking, "Active noise and vibration control-reference bibliography," III Institut der Universität Göttingen, 3. Auflage, Februar 1988.

2. J.E. Ffowcs-Williams, "Anti-sound," *Proc. R. Soc. London Ser. A* **395**, 63-88 (1984).

3. J. Scheuren, "Aktive Beeinflussung der Wellenausbreitung I. Theoretische Überlegungen zur aktive Beeinflussung der Ausbreitung von Luft- und Körperschall," *Acustica* **71**, 243-256 (1990).

4. J. Scheuren, "Aktive Beeinflussung der Wellenausbreitung II. Realisierungsmöglichkeiten einer activen Beeinflussung der Ausbreitung von Biegewellen," *Acustica* **72**, 33-46 (1990).

5. P.A.Nelson and S.J. Elliott, Active Control of Sound (Academic Limited, London, 1992).

6. R.J. Bobber, "Active load impedance," *J. Acous. Soc. Am.* **34**, 282-288 (1962).

7. R.J. Bobber, "An active transducer as a characteristic impedance of an acoustic transmission line," *J. Acous. Soc. Am.* **48**, 317-324 (1970).

8. L.G. Beatty, "Acoustic impedance in a rigid-walled cylindrical sound channel terminated at both ends with active transducers," *J. Acous. Soc. Am.* **36**, 1081-1089 (1964).

9. L.G. Beatty, R.J. Bobber, and D.L. Phillips, "Sonar transducer calibration in a high-pressure tube," *J. Acous. Soc. Am.* **39**, 48-54 (1966).

10. D. Guicking, K. Karcher, and Mathias Rollwage, "Coherent active methods for application in room acoustics," *J. Acous. Soc. Am.* **78**, 1426-1434 (1985).

11. D. Guicking, J. Melcher, and R. Wimmel, "Active impedance control in mechanical structures," *Acustica* **69**, 39-52 (1989).

12. F. Orduña-Bustamante and P.A. Nelson, "An adaptive controller for the active absorption of sound," *J. Acous. Soc. Am.* **91**, 2740-2747 (1992).

13. P.S.Dubbelday and R. Homer, "Algorithm-based method for suppressing the transmission of sound in a water-filled waveguide," *J. Intell. Mater. Syst. Struct.* **2**, 129-147 (1990).

14. P.S. Dubbelday, "Surface impedance modification of plates in a water-filled waveguide," Proceedings of the ADPA Conference on Active Materials and Adaptive Structures, G.J. Knowles, ed., Alexandria, VA, Nov. 1991, pp. 451-454.

15. L.E. Ivey, Underwater Electroacoustic Standard Transducers Catalog, Naval Research Laboratory, USRD, Orlando, FL, 1982, pp 73-77.

16. P.S. Dubbelday and C.M. Ruggiero, "Computation of propagation speed and reflection of axially symmetric waves in composite cylinders, with application to impedance tube and calibrator," NRL Memorandum Report 4885, Aug. 1982.

17. P.S. Dubbelday, "Poisson's ratio of foamed aluminum determined by laser Doppler vibrometry," *J. Acous. Soc. Am.* **91**, 1737-1744 (1992).

18. L.D. Lafleur, F.D. Shields, and J.E. Hendrix, "Acoustically active surfaces using piezorubber," *J. Acous. Soc. Am.* **90**, 1230-1237 (1991).

19. X.-Q. Bao, V.K. Varadan, V.V. Varadan, T.R. Howarth, "Model of a bilaminar actuator for active acoustic control," *J. Acous. Soc. Am.* **87**, 1350-1352 (1990).

20. M.D. McCollum, S.E. Forsythe, and A.D. McCleary, "Electromechanical modeling of an active isolation system," Proceedings of the Conference on Recent Advances in Active Control of Sound and Vibrations held at Virginia Polytechnic Inst. and State Univ. in Blacksburg, VA, on 15-17 April 1991, C.A. Fuller, Ed., Technomic, 1991, pp. 914-924.

21. B.A. Auld, Acoustic Fields and Waves in Solids (Wiley, New York, 1973), Vol. I, p. 330.

22. L.E. Kinsler and A.R. Frey, Fundamentals of Acoustics, Second ed. (Wiley, New York, 1962) p 201.

Appendix A

MODEL FOR NO-REFLECTION EXPERIMENT

BASIC EQUATIONS AND DEFINITIONS

In Fig. A1 the geometry of a plate with two active layers is shown.

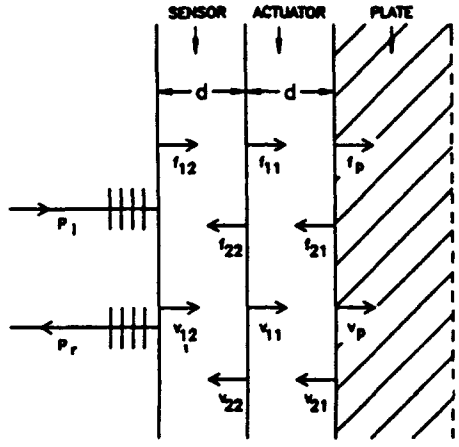

Fig.A1 Sketch of interaction of incoming wave with plate and double transducer. Surface forces per unit area are indicated by f_{ij}, surface velocities by v_{ij}. The first subscript refers to the side of a given layer: 1 for the side oriented towards the incoming wave, 2 for the opposite side. The second subscript refers to the active layer: 1 for the actuator and 2 for the sensor.

A harmonic wave with pressure p_i and angular frequency ω impinges on the sensor face. The pressure of the reflected wave is indicated by p_r. Assuming thin-plate theory, for which the thickness of the plate is small compared with the lateral dimensions, the forces per unit area f_{ij} and the velocities v_{ij} (i,j = 1,2) are related by the following set of equations [19]. The first subscript refers to the sides of a given layer: 1 for the side oriented towards the incoming wave, 2 for the opposite side. The second subscript refers to the active layers: 1 for the actuator and 2 for the sensor.

$$f_{11} = z_{11} v_{11} + z_{12} v_{21} + z_{13} J_1 \quad \text{(A1)}$$

$$f_{21} = z_{12} v_{11} + z_{11} v_{21} + z_{13} J_1 \quad \text{(A2)}$$

$$V_1 = z_{13} v_{11} + z_{13} v_{21} + z_{33} J_1 \quad \text{(A3)}$$

$$f_{12} = z_{11} v_{12} + z_{12} v_{22} \quad \text{(A4)}$$

$$f_{22} = z_{12} v_{12} + z_{11} v_{22} \quad \text{(A5)}$$

$$V_2 = z_{13} v_{12} + z_{13} v_{22} \quad \text{(A6)}$$

where

$$z_{11} = \rho c \; / \; (\; i \tan kd \;)$$

$$z_{12} = \rho c \; / \; (\; i \sin kd \;)$$

$$z_{13} = h_{33} \; / \; i \omega$$

$$z_{33} = d \; / \; (\; i \omega \epsilon_{33}^{S} \;)$$

ρ - density of solid

$$c = (\; c_{33}^{D} \; / \; \rho)^{1/2}$$

d - transducer thickness

$k = \omega \; / \; c$

J_1 - current density in actuator

V_1 - voltage across actuator,

V_2 - voltage across sensor

with the following definitions of the material coefficients:

$h = -(\partial T/\partial D)_S = -(\partial E/\partial S)_D$

$\epsilon^S = (\partial D/\partial E)_S$

$c^D = (\partial T/\partial S)_D$

D - electric displacement

E - electric field

S - strain

T - stress.

The boundary conditions are as follows:

$$f_{12} = p_i + p_r ,$$

$$v_{12} = \frac{p_i - p_r}{z_o} ,$$

$$f_{11} = f_{22} , \tag{A7}$$

and

$$v_{11} = -v_{22} ,$$

where $z_o = (\rho\ c)_{medium} = \rho_o c_o$, and c_o is influenced by the elasticity of the cylinder wall.

FIRST STEP: NO VOLTAGE IMPRESSED ON ACTUATOR

In this case the current density J_1 is zero. One solves Eqs. (A1-A6) for the variables f_{22}, f_{12}, v_{22}, v_{12}, f_{21}, v_{21}, in terms of the two voltages V_1 and V_2. The results are

$$f_{12} = \frac{z_{11}(V_1+V_2) - (z_{11}+z_{12})(V_1-V_2)}{2z_{13}} ,$$

$$v_{12} = \frac{(z_{11}-z_{12})(V_1+V_2) - z_{11}(V_1-V_2)}{2z_{13}(z_{11}-z_{12})} , \tag{A8}$$

$$f_{21} = \frac{z_{11}(V_1+V_2) + (z_{11}+z_{12})(V_1-V_2)}{2z_{13}} ,$$

and

$$v_{21} = \frac{(z_{11}-z_{12})(V_1+V_2) + z_{11}(V_1-V_2)}{2z_{13}(z_{11}-z_{12})} .$$

To simplify these results, one uses the following properties of z_{ij}:

$$z_{11} - z_{12} = i\ \rho c \tan(0.5kd) ,$$

$$z_{11} + z_{12} = -i\ \rho c \cot(0.5kd) ,$$

$$z_{11}^2 - z_{12}^2 = (\rho c)^2,$$

$$\frac{z_{11} + z_{12}}{z_{11}} = \frac{1 + \cos kd}{\cos kd}, \tag{A9}$$

$$\frac{z_{11}}{z_{11} - z_{12}} = \frac{-\cos kd}{1 - \cos kd},$$

$$\frac{z_{11} + z_{12}}{z_{11} - z_{12}} = \frac{-(1+\cos kd)}{1 - \cos kd},$$

and

$$2z_{11}^2 - z_{12}^2 = -(\rho c)^2 \frac{2\cos(2kd)}{1 - \cos(2kd)}.$$

Then

$$f_{12} = \frac{z_{11}[(V_1+V_2) - (V_1-V_2)(1 + \cos kd)/\cos kd]}{2z_{13}},$$

$$v_{12} = \frac{(V_1+V_2) + (V_1-V_2)\cos kd/(1 - \cos kd)}{2z_{13}},$$

$$f_{21} = \frac{z_{11}[(V_1+V_2) + (V_1-V_2)(1+ \cos kd)/\cos kd]}{2z_{13}}, \tag{A10}$$

and

$$v_{21} = \frac{(V_1+V_2) - (V_1-V_2)\cos kd/(1 - \cos kd)}{2z_{13}}.$$

The surface impedance of the plate z_p is found by $z_p = - f_{21}/v_{21}$ and the input impedance to the sensor surface z_e by $z_e = f_{12} / v_{12}$.

One may derive a compact expression for the non-dimensional plate impedance z_p', in the form

$$z_p' = \frac{z_p}{z_{11} - z_{12}} = \frac{(V_1+V_2)\cos kd + (V_1-V_2)(1 + \cos kd)}{(V_1+V_2)(1 - \cos kd) - (V_1-V_2)\cos kd}, \tag{A11}$$

and for the nondimensional sensor impedance z_e'

$$z_e' = \frac{z_e}{z_{11} - z_{12}} = \frac{(V_1+V_2)\cos kd - (V_1-V_2)(1 + \cos kd)}{(V_1+V_2)(\cos kd - 1) - (V_1-V_2)\cos kd} . \quad (A12)$$

Notice that z_p and z_e are not dependent on the value of h_{33}, but only on the values of ρ and c, directly in the factor $z_{11}-z_{12}$ and indirectly through the wave number $k=\omega/c$.

A further simplification is possible when kd is small, namely

$$z_p' = - \frac{3 V_1 - V_2}{V_1 - V_2} , \quad (A13)$$

and

$$z_e' = \frac{V_1 - 3 V_2}{V_1 - V_2} . \quad (A14)$$

The dimensional impedances are approximated by

$$z_p \simeq 0.5 \; i \; \omega\rho d\left[\frac{-3V_1 + V_2}{V_1 - V_2}\right], \quad (A15)$$

and

$$z_e \simeq 0.5 \; i \; \omega\rho d\left[\frac{V_1 - 3V_2}{V_1 - V_2}\right]. \quad (A16)$$

Thus, for small kd the results for z_p and z_e depend only on ρ and d, which are easily determined quantities.

Notice that for $z_p = 0$, i.e., the actuator without backing plate and exposed to air, one has $V_2 = 3V_1$, and thus $z_e \simeq i \; \omega\rho(2d)$, expressing the fact that, for small kd, the input impedance is just the inertia of the double transducer in this case.

SECOND STEP: SOLUTION WHEN z_p IS GIVEN

In the second step of the no-reflection experiment the plate impedance z_p is known from the results of the first step. One enters the relations $f_{11} = f_{22}$, $v_{11} = - v_{22}$ and $f_{21} = - z_p v_{21}$ into the six Eqs. (A1-A6), and solves for the variables f_{12}, f_{22}, v_{22}, v_{12}, v_{21}, J_1, in terms of V_1, V_2, and z_p.

One introduces two quantities k_1^2 and k_1^2 by $k_1^2 = z_{13}^2/z_{11}z_{33}$ and $k_2^2 = z_{13}^2/z_{12}z_{33}$. For small kd one has $k_1^2 \simeq k_2^2 \simeq k_t^2$, where k_t is the thickness coupling constant, $k_t^2 = h_{33}^2 \epsilon_{33}^S / c_{33}^D$.

The results are expressed in compact form, by again using z_p', the non-dimensional impedance. The denominator D is the same for all variables;

$$\frac{D}{z_{13}^2(z_{11}-z_{12})} = z_p' \left[1 - \frac{2}{k_1^2} + \frac{1}{k_2^2}\right] + \left[3 - \frac{2}{k_1^2} - \frac{1}{k_2^2}\right] . \qquad \text{(A17)}$$

Only the expressions for f_{12} and v_{12}, needed to compute the input impedance to the sensor $z_e = f_{12}/v_{12}$, are given here;

$$\frac{Df_{12}}{z_{13}(z_{11}-z_{12})^2} = V_1(1 + z_p') + V_2\left\{1 - \frac{2(1-1/k_1^2)(1 + \cos kd)}{1 - \cos kd}\right.$$

$$\left. + z_p'\left[\frac{(1-1/k_1^2)\cos kd}{1 - \cos kd} - \left(\frac{1}{k_1^2} + \frac{1}{k_2^2}\right)\right]\right\} ,$$

and (A18)

$$\frac{Dv_{12}}{z_{13}(z_{11}-z_{12})} = V_1(1+z_p') + V_2\left[2 - \frac{(1-1/k_1^2)\cos kd}{1 - \cos kd}\right.$$

$$\left. + -\left(\frac{1}{k_1^2} + \frac{1}{k_2^2}\right) + z_p'\left[1 - \frac{2}{k_1^2}\right]\right] .$$

For $kd \ll 1$, and $k_1^2 \simeq k_2^2 \simeq k_t^2 \ll 1$, one has

$$\frac{D}{z_{13}^2(z_{11}-z_{12})} \simeq \frac{-1}{k_t^2}\,(3+z_p'),$$

$$\frac{Df_{12}}{z_{13}(z_{11}-z_{12})_2} \simeq V_1(1+z_p') + V_2\,\frac{8+2z_p'}{(kd\,k_t)^2}\,, \tag{A19}$$

and

$$\frac{Dv_{12}}{z_{13}(z_{11}-z_{12})} \simeq V_1(1+z_p') + 2V_2\,\frac{1/(kd)^2 - z_p'}{k_t^2}\,.$$

These expressions show that, although $V1 \gg V_2$, V_2 is divided by the small quantities $(kd)^2$ and k_t^2, and thus the term with V_2 may be of the same order of magnitude, or larger than the term with V_1. Thus, it is necessary to know $(kd)^2$ and k_t^2 to sufficient accuracy, including the imaginary part of k_t.

(BLANK PAGE)

Appendix B

FIGURE(S)-OF-MERIT IN NO-REFLECTION EXPERIMENT

In order to derive figure(s)-of-merit (FOM) one requires a different solution of the same basic equations, where now the voltages V_1 and V_2 are unknown. These solutions may also serve to estimate the expected or necessary voltages for sensor and actuator, respectively, to predict the measurement values in a given experiment.

In the first part of the experiment one determines z_p from the measured V_1 and V_2, while $J_1 = 0$. One solves Eqs. (A1-A6) for V_1, V_2, f_{22}, v_{22}, v_{21}, and v_{12}, in terms of f_{12}, introducing a non-dimensional impedance z_p by $z_p' = z_p / (z_{11} - z_{12})$. Then

$$V_1 = \frac{f_{12} z_{13}}{z_{11}} \quad \frac{1 + z_p'}{2(1 + z_p') \cos kd + (2 - z_p'/\cos kd)} , \tag{B1}$$

and

$$V_2 = \frac{f_{12} z_{13}}{z_{11}} \quad \frac{2 \cos kd \, (1 + z_p') + (1 - z_p')}{2(1 + z_p') \cos kd + (2 - z_p'/\cos kd)} . \tag{B2}$$

To reduce the signal-to-noise ratio the voltages should be as large as possible. One sees that for a given incoming wave, represented by f_{12}, the two voltages will be proportional to the ratio z_{13}/z_{11}, which therefore may serve as a FOM.

For small values of kd this FOM simplifies to

$$FOM = \frac{h_{33} d}{c_{33}^D} . \tag{B3}$$

Thus, for small kd one may write:

$$\frac{V_1}{f_{12}} = \text{FOM}\,\frac{1 + z_p'}{4 + z_p'},$$

and (B4)

$$\frac{V_2}{f_{12}} = \text{FOM}\,\frac{3 + z_p'}{4 + z_p'}.$$

The ratio V_2/V_1 varies from 3 for $z_p'=0$ to 1 for $z_p' \to \infty$.

Not surprisingly (see Ref. 22), the other variables may be expressed as follows:

$$\frac{f_{11}}{v_{11}} = -\frac{f_{22}}{v_{22}} = \rho c\,\frac{i\,\rho c \tan kd + z}{\rho c + i\,z_p \tan kd}. \tag{B5}$$

For small kd, this reduces to the impedance $i\rho\omega d\,(1 + z_p'/2)$.

Similarly,

$$z_e = \frac{f_{12}}{v_{12}} = \rho c\,\frac{i\,\rho c \tan 2kd + z_p}{\rho c + i z_p \tan 2kd}. \tag{B6}$$

Further,

$$\frac{f_{22}}{f_{12}} = \frac{1 + \cos kd(1+z_p')}{2\cos kd\,(1+\cos kd) + z_p'\,(2\cos^2 kd - 1)}. \tag{B7}$$

For small kd this reduces to

$$\frac{f_{22}}{f_{12}} = \frac{2 + z_p'}{4 + z_p'}. \tag{B8}$$

The ratios of the other velocities to v_{22} are

$$\frac{v_{21}}{v_{22}} = [\cos kd + z_p'(\cos kd - 1)]^{-1}, \tag{B9}$$

and

$$\frac{v_{12}}{v_{22}} = \frac{2z_p' \cos kd(1-\cos kd) + 1 - 2\cos^2 kd}{\cos kd + z_p'(\cos kd - 1)} \quad . \tag{B10}$$

For small kd these ratios reduce to 1 and -1, respectively.

In the second part of the no-reflection experiment the value of z_p is given, and the value of the voltage on the actuator is adjusted to reach the desired z_e. Again, in order to improve the signal-to-noise ratio one wants to optimize the voltage V_2, given f_{12}. Introducing a non-dimensional input impedance by $z_e' = z_e / (z_{11} - z_{12})$, one finds by solving the Eqs.(A1-A6) for V_1, V_2, f_{22}, v_{22}, v_{21}, and J_1, in terms of f_1,

$$V_2 = \frac{z_{13}\, f_{12}}{z_{12}} \, \frac{z_e' - 1}{z_e'} \quad . \tag{B11}$$

Thus, one finds here for a FOM the ratio z_{13} / z_{12}, which, for small kd, reduces to the same value for the FOM as in the first part of the experiment.